SciEn

*Proceedings of 8th International Conference on Mechanical, Industrial and Energy Engineering 2024*
*02-04 January, 2025, Khulna, BANGLADESH*

SciEn Conference Series: Engineering Vol. 3, 2025, pp 92-95 https://doi.org/10.38032/scse.2025.3.20

# Synthesis and Characterization of $SiO_2$ Coated $Fe_3O_4$ Nanoparticles by Co-precipitation Method

*Shamima Akhter Urmi**, *M. Bodiul Islam, M. Mosiul Haque, M. Sadman Shahriar, Abdullah Al Mahmood*

Nano Synthesis Laboratory, Department of Glass & Ceramic Engineering, Rajshahi University of Engineering & Technology, Rajshahi – 6204, Bangladesh

**ABSTRACT**

This research investigated the structural and morphological characteristics of $Fe_3O_4$ nanoparticles (NPs), coated with a $SiO_2$ shell, produced by co-precipitation method. Triethanolamine (TEA), cetyltrimethylammonium bromide (CTAB), ammonium hydroxide ($NH_4OH$), iron salt ($FeCl_2.4H_2O$, $FeCl_3.6H_2O$), and tetraethyl orthosilicate (TEOS) are the precursors to form nanoparticles with a magnetite core coated with silica ($SiO_2$). The drying temperature was 40 °C and then the sample was calcined at 550 °C temperature to enhance crystallinity and form a stable core-shell structure. The stability and surface functionality of magnetite ($Fe_3O_4$) nanoparticles introduces versatile materials with an extensive variety of uses. X-ray diffraction (XRD) confirmed the crystalline structure with distinct sharp peaks corresponding to $Fe_3O_4$-$SiO_2$ phases with average crystallite size of 8.459 nm, and scanning electronic microscopy (SEM) revealed the narrow particle size distribution and exhibiting a spherical morphology. The calculated optical band gap of 3.21 eV represented its usage in optoelectrical field. The prevention from agglomeration and enhanced stability are the benefits of the core-shell nanostructured materials which has made them acting as effective adsorbent in environmental applications such as wastewater treatment, rapid magnetic separation and also in biomedical applications and drug delivery systems.

Keywords: Co-precipitation, Nanoparticles, XRD, SEM, Band gap.



## 1. Introduction

The family of magnetic iron oxide nanoparticles (MIONs), which has unique magnetic properties, are electromagnetic radiation adsorbent materials (i.e. incident electromagnetic radiation is absorbed and converted into thermal energy) [1]. These iron oxides are magnetite ($Fe_3O_4$), maghemite ($\gamma$-$Fe_2O_3$), and hematite ($\alpha$-$Fe_2O_3$). $Fe_3O_4$ indicates inverse spinel crystal structure, and the tetrahedral sites are filled with half of $Fe^{3+}$ ions whereas the octahedral sites are filled with $Fe^{2+}$ and other half of $Fe^{3+}$ ions with the same proportions [2]. The unique properties of iron oxides make them suitable in numerous applications e.g. magnetic resonance imaging, drug delivery and environmental remediation [3]. However, the general issues with iron oxide nanoparticles is prone to oxidation and agglomeration. To mitigate these challenges, use of surface functionalizing agent is the best choice as it improves the surface stability and biocompatibility of magnetic nanoparticles providing outer shell on the surface of the magnetic iron oxide nanoparticles [4]. Furthermore, several methods are available to prepare $Fe_3O_4$ nanoparticles (NPs) conducting with $H_2$ annealing at a certain temperature which is difficult to control, highly cost-effective, and very dangerous. Moreover, hydrothermal, sol-gel, thermal decomposition, hydrolysis technique is another route [5-7]. An inert atmosphere is the best choice for calcining at 550 °C and forming the desired product. However, their high surface energy tends to agglomerate and lose their properties in biomedical applications. To prevent these challenges, surface functionalization with mesoporous silica ($SiO_2$) is one of the promising approaches as silica is safe for biomedical applications as well as have good thermal stability, mechanical strength and low specific weight for high-temperature treatment up to 1000 °C, energy to waste management, waste water-treatment [8-9]. Other applications are electronics, optics, biomedicine, magnetic nano-vectors, hyperthermia, therapeutic tools, and enhancing the ability of MRI-based imaging and cellular systems [9]. When industrial waste, battery manufacturing industries, electroplating, and plastic are dumped into the water, it contaminates and contains heavy metals e.g. lead (Pb), chromium (Cr), etc. The utilization of iron oxide nanomaterials as adsorbent has been received much more attention as these NPs degrade the heavy metal and catalysis properties [10]. This work's goal is to prepare the nanoparticles of $Fe_3O_4$-$SiO_2$ and to prevent the fabricated nanoparticles from getting oxidized and agglomeration, which is a serious issue working with iron oxide nanoparticles. This problematic issue was solved by applying a thin layer of silica that keep the outer surface of iron oxide nanoparticles away from the air. Additionally, a cost-effective fabrication route was used at moderate temperature in presence of continuous flow of nitrogen at self-made laboratory setup. The structural and morphological effect of $SiO_2$ as a functionalizing agent was evaluated using XRD, SEM-EDS. Besides, Optical band gap was determined by UV-Vis spectroscopy.

*Corresponding Author Email Address: urmi@gce.ruet.ac.bd Published By: SciEn Publishing Group

## 2. Methodology

### 2.1 Materials

For the synthesis process, the required materials are: iron (II) chloride tetrahydrate ($FeCl_2.4H_2O$), iron (III) chloride hexahydrate ($FeCl_3.6H_2O$), cetyltrimethylammonium bromide (CTAB: $[(C_{16}H_{33})N(CH_3)_3]Br$), $NH_4OH$ (28%), tetraethyl orthosilicate (TEOS: $Si(OC_2H_5)_4$), triethanolamine (TEA: $C_6H_{15}NO_3$), and deionized water. All the materials used were of analytical grade and applied without further purification.

### 2.2 Method

In this precipitation method, magnetic nanoparticles were synthesized in the ammonium hydroxide solution with iron chloride salts. Then, through the sol-gel process, CTAB, TEA surfactants, and TEOS were added to the solution and formed a core-shell structure. Initially, deionized water of 100 ml was heated to 80 °C in a flask in presence of nitrogen atmosphere, and oxygen was removed at 1200 rpm by homogenizing for 10 minutes. Then 0.4 gm of $FeCl_2.4H_2O$ and 0.9 gm of $FeCl_3.6H_2O$ were added and stirred in the same conditions. 20 ml of ammonium hydroxide solution was added, and a coprecipitation reaction occurred. For this, magnetite nanoparticles formed, and the caramel color turned black. Mixing continued for 10 minutes, and then concentrations of 1.5 gm of CTAB were added and stirred for 5 minutes. The reaction was continued for 10 minutes by adding 0.8 ml of TEA. Finally, the sol-gel process was initiated after 1.0 ml of TEOS were added and continued the process for 10 minutes. The synthesized product was collected after being centrifuged. Deionized water was used to wash the nanoparticles for several times. Afterwards at 40 °C, it was dried in an oven and calcined in a furnace at 550 °C for six hours to remove CTAB. The synthesized powder was analyzed using x-ray diffraction (XRD), scanning electron microscopy (SEM) and UV-Vis spectroscopy.

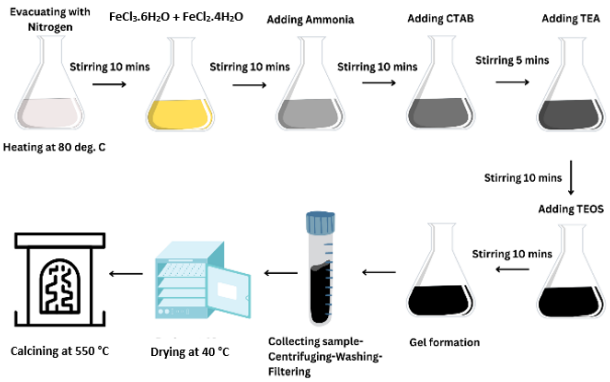


**Fig.1** Process flow diagram of $Fe_3O_4$ nanoparticles coated with silica.

## 3. Characterization

### 3.1 XRD

The crystallite size of the synthesized nanoparticles is calculated using Debye-Scherer's equation,

$$D = \frac{k\lambda}{\beta cos\theta} \quad (1)$$

The full width at half maximum (FWHM) of the peak, expressed in radians ($2\pi$), is represented by 'β', 'k' denotes the crystallite shape factor (0.89), and 'θ' denotes the peak position. Furthermore, the following relation was used to determine the lattice parameters (a and c),

$$\frac{1}{d^2} = \frac{h^2+k^2}{a^2} + \frac{l^2}{c^2} \quad (2)$$

### 3.2 UV-Visible Spectroscopy

The optical properties of the synthesized nanoparticles are investigated using UV-Vis spectroscopy [11]. Tauc and Devis Mott relation is used to probe the absorption spectroscopy. In this equation,

$$\alpha h\nu = k\,(h\nu - E_g) \quad (3)$$

Where, hν = Incident photon energy, K = Energy independent constant,

## 4. Results and Discussion

### 4.1 XRD Analysis

The crystallinity of the $Fe_3O_4$-$SiO_2$ nanoparticles calcined at 550 °C in 6 hours is observed through x-ray diffraction (Fig.2). The average crystallite size is calculated as 8.459 nm (Table 1) using the formula of Debye-Scherer's equation (Eq.1). All of the peaks correspond to the standard XRD patterns of $Fe_3O_4$ [JCPDs card no. 96-900-6323], which include $2\Theta$ = 30.50, 35.88, 43.61, 54.05, 57.64, 63.20, and their corresponding lattice indices are [220], [311], [400], [422], [511], [440]. In addition, the presence of these planes confirms the cubic spinel structure. Again, the peak observed between 22 and $30^0$ confirms the presence of $SiO_2$ phase. Therefore, the peaks obtained for both $SiO_2$ and magnetite confirms that the prepared sample is magnetite nanoparticles coated with $SiO_2$ [12]. Table 2 represents the calculated density and unit cell volume of 5.07 g/cm$^3$ and 587.22×10$^6$ pm$^3$ respectively.

**Table 1** Crystallite size calculated from XRD.

| ($2\theta$) | FWHM | Crystallite size D (nm) | Average (nm) |
|---|---|---|---|
| 30.5071 | 0.82489 | 9.2914 | 8.4594 |
| 35.8830 | 0.8702 | 8.6853 | |
| 43.6153 | 0.82384 | 8.9529 | |
| 54.0558 | 0.79763 | 8.8721 | |
| 57.6487 | 0.8837 | 7.8759 | |
| 63.2072 | 0.95577 | 7.0792 | |

**Table 2** Parameter analysed by XRD results.

| Lattice parameter | | c/a | Crystal System | Unit cell volume ($10^6$ pm$^3$) | Calculated Density (g/cm$^3$) |
|---|---|---|---|---|---|
| a | c | | | | |
| 8.374 | 8.374 | 1 | Cubic | 587.22 | 5.07 |

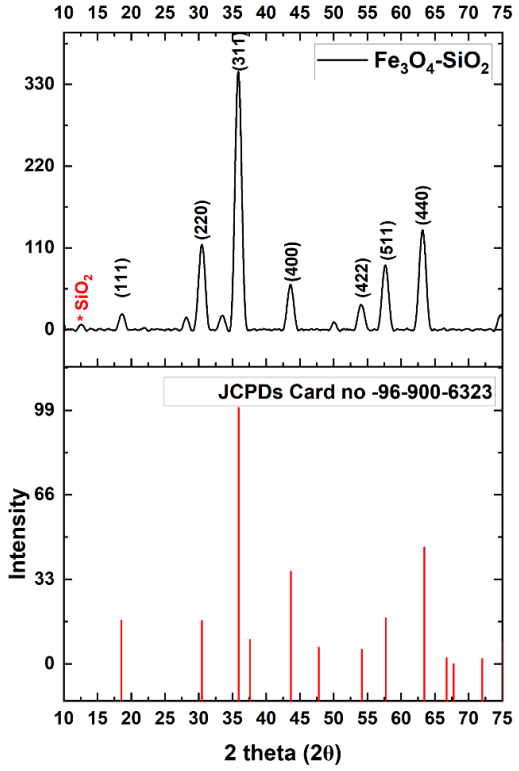


**Fig.2** XRD pattern for $Fe_3O_4$ nanoparticles coated with $SiO_2$.

### 4.2 SEM Analysis

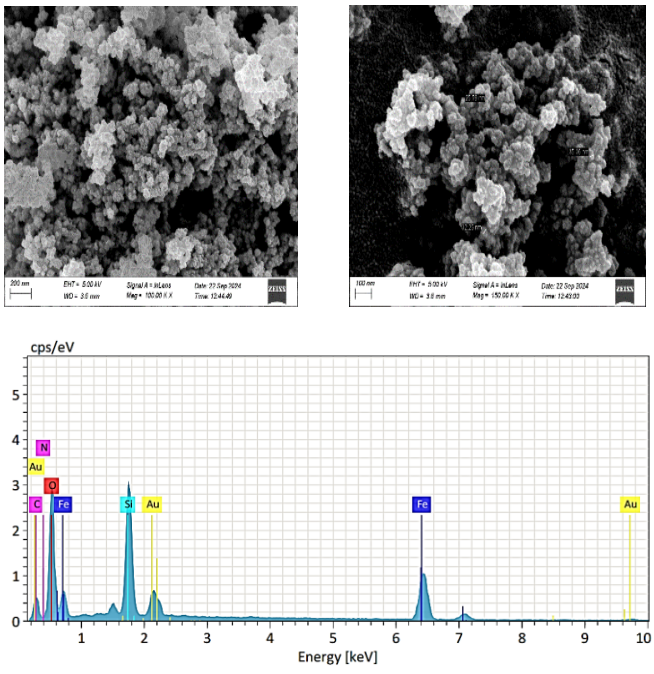


**Fig.3** Scanning electron micrograph, and EDS results for $Fe_3O_4$ nanoparticles coated with $SiO_2$.

To analyze the nanoparticles, scanning electron microscopy (SEM) technique was used, as shown in the Fig.3. EDS result (Fig.3) confirms the presence of $SiO_2$ and iron oxide in the synthesized sample. As seen in the micrographs, the structure is composed of highly porous and the particles get clumped together. The aggregated particles form dense clusters and signify the existence of interconnected voids which might influence the effective surface area and adsorption capacity. In Fig.4, the diameter distribution mean value is 92.3 nm. From the observation, it can be noticed that the diameter of the nanoparticles has a slight variation. In the Fig.3, more widespread cluster forms, that extend across the surface, which gives additional proof of structural homogeneity. A strong adsorption potential is indicated by the porous and rough surface which promotes interaction between the material and target molecules [12].

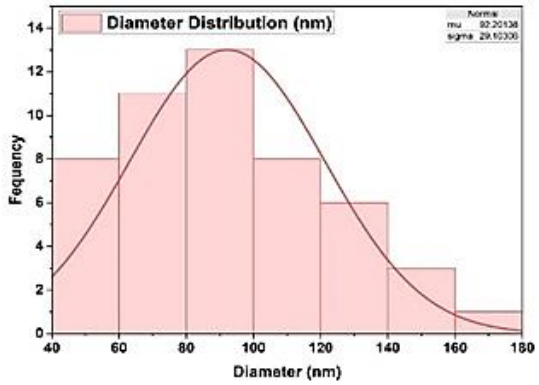


**Fig.4** Particle size distribution of $Fe_3O_4$ nanoparticles coated with silica.

### 4.3 UV-Visible Spectroscopy Analysis

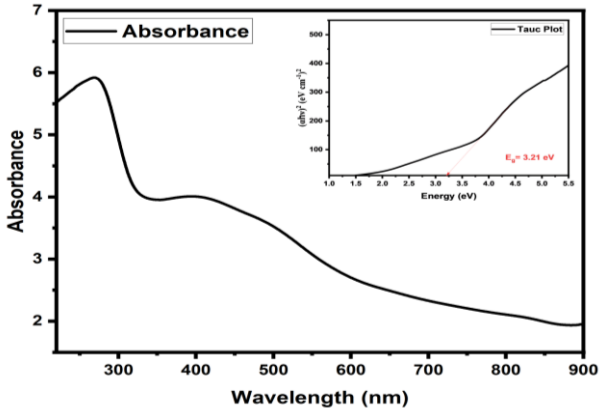


**Fig.5** Tauc plot for band gap energy of $Fe_3O_4$ nanoparticles coated with silica.

From the Tauc plot, the obtained band gap is 3.21 eV for the nanoparticles of $Fe_3O_4$ coated with silica. These nanoparticles show the insulating properties [13]. The absorbance spectrum was recorded over the wavelength range of 200 to 1000 nm. The absorbance peak around 300 nm shows that there is strong absorption in the ultraviolent region, which attributes the electrical transition to the material's structure, such in between the valence band and conduction band. The graph shows a gradual decline in absorbance towards the visible region, and a high degree of

transparency in 400 nm. The material reduces absorbance in the visible region and have limited interaction with light. The Tauc plot determines the band gap energy of the sample and the optical band gap of the sample is calculated as approximately 3.21 eV. This result indicates the prepared sample as a semiconductor with a direct band gap. The UV-Vis analysis along the Tauc plot confirmed its optoelectrical application consistent with typical semiconductors [13].

## 6. Conclusion

This research was based on the synthesis of the magnetite nanoparticles with silica core-shell by the co-precipitation method, progressing in XRD and SEM results. An inert atmosphere was the prerequisite to synthesize NPs for mitigating their oxidation. From the XRD result, crystalline phase with cubic spinel structure was determined and the average crystallite size was 8.459 nm. The SEM result declared the distribution in particle size. The presence of $Fe_3O_4$ and $SiO_2$ was observed from EDS. Optical band gap of 3.21 eV of the prepared nanoparticles represented their semiconducting nature that is useful in optoelectrical application.

## 5. Acknowledgement

The authors like to pay their gratitude to the Rajshahi University of Engineering & Technology for providing the facilities to conduct this research.

## References

[1] A. M. G. Silva, I. M. Pereira, T. I. Silva, M. R. da Silva, R. A. Rocha, and M. C. Silva, “Magnetic foams from polyurethane and magnetite applied as attenuators of electromagnetic radiation in X band,” *J Appl Polym Sci*, vol. 138, no. 1, Jan. 2021, doi: 10.1002/app.49629.

[2] V. Gurenko, L. Gulina, and V. Tolstoy, “Sol–gel–xerogel transformations in the thin layer at the salt solution–gaseous reagent interface and the synthesis of new materials with microtubular morphology,” *J Solgel Sci Technol*, vol. 92, no. 2, pp. 342–348, Nov. 2019.

[3] S. Pan, W. Huang, Y. Li, L. Yu, and R. Liu, “A facile diethyl-carbonate-assisted combustion process for the preparation of the novel magnetic α-$Fe_2O_3$/$Fe_3O_4$ heterostructure nanoparticles,” *Mater Lett*, vol. 262, Mar. 2020.

[4] Y. O. Olaseni, Nanostructured Magnetite Coated by Natural Product Extracts to Remove Heavy Metal Ions and Inactivate Bacteria. M.S. thesis, Texas A&M University-Kingsville, Kingsville, TX, USA, May 2020.

[5] A.G. Roca, M.P. Morales, K. O'Grady, C.J. Serna, Structural and magnetic properties of uniform magnetite nanoparticles prepared by high temperature decomposition of organic precursors, Nanotechnology 17 (2006) 2783–2788.

[6] H. Iida, K. Takayanagi, T. Nakanishi, T. Osaka, Synthesis of $Fe_3O_4$ nanoparticles with various sizes and magnetic properties by controlled hydrolysis, J. Colloid Interface Sci. 314 (2007) 274–280.

[7] D. Maity, S.-G. Choo, J. Yi, J. Ding, J.M. Xue, Synthesis of magnetite nanoparticles via a solvent-free thermal decomposition route, J. Magn. Magn. Mater. 321 (2009) 1256–1259.

[8] F. Morales, V. Sagredo, T. Torres, G. Márquez, Characterization of magnetite nanoparticles synthesized by the coprecipitation method, Cienc. e Ing. 40 (2019) 39–44.

[9] K. Faaliyan, H. Abdoos, E. Borhani, and S. S. S. Afghahi, “Core-shell nanoparticles for medical applications: effects of surfactant concentration on the characteristics and magnetic properties of magnetite-silica nanoparticles,” *Nanomed J*, vol. 6, no. 4, pp. 269–275, Oct. 2019.

[10] M. Namvar-Mahboub, E. Khodeir, M. Bahadori, and S. M. Mahdizadeh, “Preparation of magnetic MgO/$Fe_3O_4$ via the green method for competitive removal of Pb and Cd from aqueous solution,” *Colloids Surf A Physicochem Eng Asp*, vol. 589, Feb. 2020.

[11] H. Qi, B. Yan, W. Lu, C. Li, and Y. Yang, "A Non-Alkoxide Sol-Gel Method for the Preparation of Magnetite ($Fe_3O_4$) Nanoparticles," *Current Nanoscience*, vol. 7, no. 3, pp. 381-388, 2011.

[12] F. Morales, G. Márquez, V. Sagredo, T. E. Torres, and J. C. Denardin, “Structural and magnetic properties of silica-coated magnetite nanoaggregates,” *Physica B Condens Matter*, vol. 572, pp. 214–219, Nov. 2019.

[13] Z. I. Takai, M. K. Mustafa, S. Asman, and K. A. Sekak, "Preparation and Characterization of Magnetite ($Fe_3O_4$) Nanoparticles by Sol-Gel Method," *International Journal of Nanoelectronics and Materials*, vol. 12, no. 1, pp. 37-46, Jan. 2019.

## NOMENCLATURE

| | | |
|---|---|---|
| $D$ | : | Crystallite size, nm |
| $\lambda$ | : | X-ray Wavelength, nm |
| $\theta$ | : | Bragg’s Diffraction angle |
| $h$ | : | Planck's constant, J·Hz$^{-1}$ |
| $E_g$ | : | Optical band gap energy, eV |
| $\alpha$ | : | Absorption coefficient |